Proceedings of the 2004 IEEE
International Conference on Robotics & Automation
New Orleans, LA • April 2004

Impedance matching for a serial link manipulator

Ryo Kurazume
Kyushu University
6-10-1, Hakozaki, Higashi-ku, Fukuoka, Japan
Email: kurazume@is.kyushu-u.ac.jp

Tsutomu Hasegawa
Kyushu University
6-10-1, Hakozaki, Higashi-ku, Fukuoka, Japan
Email: hasegawa@irvs.is.kyushu-u.ac.jp

Abstract— **We propose a new index for dynamic performance analysis of serial link manipulators named Impedance Matching Ellipsoid, or IME. Several indexes have been proposed for indicating static and dynamic performance of robot manipulators. For example, Dynamic Manipulability Ellipsoid (DME) characterizes distributions of hand acceleration produced by normalized joint torque. Manipulating-Force Ellipsoid (MFE) denotes static torque-force transmission ef£ciency from actuators at joints to a hand. On the other hand, the proposed IME characterizes dynamic torque-force transmission ef£ciency from actuators at joints to a load held at the hand of the manipulator. The IME includes a wide range of concepts proposed so far as measures of manipulator's performance. The DME and the MFE are both derived from the IME as limiting forms about the load mass. In this paper, we demonstrate the IME with some numerical examples including the selection of an optimal leg posture for jump robots, optimum active stiffness control, and an extension for manipulators mounted on satellites in outer space.**

I. Introduction

A variety of indexes which indicate the performance of robot manipulators were proposed from the middle of 1980's to the beginning of 1990's. For indexing the static performance of robot manipulators, the Manipulability Ellipsoid (ME) [1] was introduced indicating the relationship between angular velocity at each joint and linear and angular velocity at a hand of the manipulator. Several different indexes in this category were also introduced: The Manipulating-Force Ellipsoid (MFE) [2] indicates static torque-force transmission from the joints to the hand; the compatibility index [3] for determining an optimal posture for particular tasks; the condition number of the Jacobian matrix. In addition, for indexing dynamic performance of robot manipulators, the Dynamic Manipulability Ellipsoid (DME) [4],[2],[5] was proposed describing distributions of possible hand acceleration. Another measure is the acceleration radius [6], which is obtained as the minimum value of upper boundaries of feasible hand acceleration in task space. Furthermore, the generalized inertial ellipsoid [7] which enables us to handle the distributed mass system of the manipulator as the single point mass system at the hand was proposed.

These various indexes denote static and dynamic performance of manipulators themselves, speci£cally, in the case that they are manipulated under a no-load condition. However, in some cases, we'd like to know the performance when they carry loads in the hands. Especially, in the case that loads are limited to a small variations such as pick-and-place tasks in assembly processes, the index which takes the effect of loads into account is convenient.

For an actuator and gear system, the idea of "impedance matching" has been widely used. This concept is usually utilized for the choice of the optimum gear ratio in terms of the transmission performance from torque produced at the actuator to torque applied to the load. The £tness of inertial properties between the actuator system including inertia of a rotor and the load determines the performance of torque transmission.

On the other hand, the Jacobian matrix indicates the transformation between displacements of joint angles and position of the hand of robot manipulators. Since this matrix can be regarded to correspond with the gear ratio of the actuator system mentioned above, it is possible to extend the concept of "impedance matching" to serial link manipulators. This new concept, namely, the impedance matching for serial link manipulators, can be considered as the transmission ef£ciency of torque produced at each joint to force applied to the load at the hand of the manipulator. Its performance is determined depending on the posture of the manipulator.

In this paper, we propose a new concept named "the impedance matching for serial link manipulators"[8] and a new index for indicating manipulator's dynamic performance named Impedance Matching Ellipsoid, or IME. The proposed IME characterizes the dynamic torque-force transmission ef£ciency from actuators at joints to the load held at the hand of the manipulator. The IME includes a wide range of concepts proposed so far as measures of manipulator's performance. The DME and the MFE, which have been considered as indexes which are based on distinct concepts [2], are both derived from the IME as limiting forms about the load mass. This paper demonstrates the use of the IME with two numerical examples; the selection of an optimal leg posture for jump robots and an extension to manipulators mounted on satellites in outer space.

II. Impedance matching for serial link manipulators

A. Impedance matching for actuator systems

In this section, we introduce the basic idea of the impedance matching for actuator systems. Let the moment of inertia of the actuator including a rotor and a shaft be I_m, the moment of inertia of the load be I_lCthe gear ratio be ξ, and the angular velocity of the load be ω_l as shown in Fig.1. The equivalent

torque produced by the actuator around the shaft, τ_m, can then be written as

$$\tau_m = \left(I_m + \frac{I_l}{\xi^2} \right) \xi \dot{\omega}_l \tag{1}$$

and the torque applied to the load, τ_l, is given as

$$\tau_l = I_l \dot{\omega}_l \tag{2}$$

Therefore, the transmission ef£ciency from torque produced at the actuator to torque applied to the load can be de£ned as

$$\eta = \frac{\tau_m}{\tau_l} = \frac{\left(I_m + \frac{I_l}{\xi^2} \right) \xi \dot{\omega}_l}{I_l \dot{\omega}_l} \tag{3}$$

Thus, the optimum gear ratio that maximizes the transmission ef£ciency obtained above is determined as

$$\xi = \sqrt{\frac{I_l}{I_m}} \tag{4}$$

By choosing the optimum gear ratio obtained in Eq.(4), a large acceleration of the load is produced with a small output of torque at the actuator. This idea is called as the impedance matching of actuator systems.

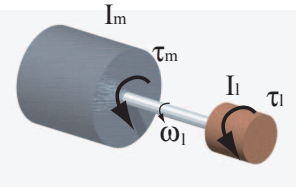

Fig. 1. Impedance matching of an actuator

B. Impedance matching for serial link manipulators

In this section, we extend the idea of the impedance matching of actuator systems to serial link manipulators. The derived index indicates the ef£ciency of torque-force transmission from actuators at each joint to the load held at the hand of the manipulator. For illustrating the idea of the impedance matching for serial link manipulators more clearly, Impedance Matching Ellipsoid, or IME, is also proposed.

The motion equation of serial link manipulators which consist of N joints and N links is written as the following equation.

$$\tau = M(q)\ddot{q} + C(q, \dot{q}) + G(q) + J(q)^T F_e \tag{5}$$

where $\tau \in R^{N \times 1}$ is joint torque, $M(q) \in R^{N \times N}$ is a tensor of inertia of the manipulator in joint space, $C(q, \dot{q}) \in R^N$ is coriolis and centrifugal forces, $G(q) \in R^N$ is gravity force, $J(q) \in R^{M \times N}$ is the Jacobian matrix, and $F_e \in R^M$ is external force and moment applied to the hand. Here, M shows the degree of freedom of the manipulator hand.

On the other hand, the motion equation of the load held at the hand is given as

$$\begin{aligned} F_e &= M_p \ddot{x} + M_p \begin{pmatrix} g \\ 0 \end{pmatrix} \\ &= M_p \ddot{x} + M_p \mathbf{g} \end{aligned} \tag{6}$$

where $\ddot{x} \in R^M$ is acceleration of the hand, $M_p \in R^{M \times M}$ is load mass, and $g \in R^M$ is acceleration of gravity. Moreover, acceleration of the hand can be obtained as

$$\ddot{x} = J(q)\ddot{q} + \dot{J}(q)\dot{q} \tag{7}$$

Since load mass M_p is a regular matrix and by substituting Eqs.(6) and (7) into Eq.(5), we get the motion equation in terms of external force and moment as follows:

$$\begin{aligned} \tau &= M(q)J(q)^\dagger M_p^{-1}(F_e - M_p\mathbf{g} - M_p\dot{J}(q)\dot{q}) \\ &\quad + C(q, \dot{q}) + G(q) + J(q)^T F_e \\ &= Q(q)(F_e - F_{bias}) \end{aligned} \tag{8}$$

where

$$\begin{aligned} F_{bias} &= (J(q)^T + M(q)J(q)^\dagger M_p^{-1})^\dagger \\ &\quad [M(q)J(q)^\dagger(\mathbf{g} + \dot{J}(q)\dot{q}) - C(q, \dot{q}) - G(q)] \end{aligned} \tag{9}$$

$$Q(q) = J(q)^T + M(q)J(q)^\dagger M_p^{-1} \tag{10}$$

and $J(q)^\dagger \in R^{M \times N}$ is a pseudo inverse of the Jacobian matrix $J(q)$. $J(q)^\dagger$ can be obtained by the following equation in the case that the Jacobian matrix is not a regular matrix.

$$J(q)^\dagger = W^{-1}J^T(JW^{-1}J^T)^{-1} \tag{11}$$

where W is a weight matrix.

Eq.(8) denotes the relationship between torque produced at actuators and force and moment applied to the load from the hand. The coef£cient matrix, $Q(q) \in R^{N \times M}$, indicates the torque-force transmission ef£ciency, and F_{bias} is a bias term related to current velocity and gravitation. Thus, by applying the singular value decomposition for this matrix $Q(q)$, we get

$$Q(q) = U\Sigma V^T \tag{12}$$

where $\Sigma = diag(\sigma_1, \sigma_2, \cdots, \sigma_M) \in R^{M \times N}$, and $U \in R^{M \times M}, V \in R^{N \times N}$ are orthogonal matrixes. Therefore, transmission ef£ciency from torque produced at each joint to force and moment applied to the load from the hand can be described by the following equation.

$$w = \sigma_1 \cdot \sigma_2 \cdots \sigma_M \tag{13}$$

In this paper, we de£ne the value of w in Eq.(13) as an index which indicates the degree of impedance matching for serial link manipulators.

C. Impedance matching ellipsoid

In this section, we assume that torque limits at each actuator are symmetrical, namely,

$$-\tau_i^{limit} \leq \tau_i \leq \tau_i^{limit} \tag{14}$$

Let's consider a conversion matrix, L

$$L = diag(\tau_1^{limit}, \tau_2^{limit}, \cdots, \tau_n^{limit}) \tag{15}$$

Then, normalized joint torque is obtained with L as

$$\tilde{\tau} = L^{-1}\tau \tag{16}$$

where $\tilde{\tau}$ is normalized torque. Therefore, when the normalized torque with the magnitude of 1 is produced, force and moment applied to the load are derived from

$$\tilde{\tau}^T \tilde{\tau} \leq 1 \tag{17}$$

as

$$(F_e - F_{bias})^T Q^T L^{-2} Q (F_e - F_{bias}) \leq 1 \tag{18}$$

This equation indicates the ellipsoid of transmitted force and moment from joints to the load, and thus, we de£ne this ellipsoid as Impedance Matching Ellipsoid, or IME.

D. Features of the IME

The IME de£ned Eq.(18) coincides with Dynamic Manipulability Ellipsoid (DME) in the case that $M_p \rightarrow 0$, and Manipulating-Force Ellipsoid (MFE) in the case that $M_p \rightarrow \infty$. We will show this relation in this section.

At £rst, we assume that $M_p \rightarrow 0$. Then, since $F_e = 0$ from Eq.(6), Eq.(8) can be rewritten as

$$\begin{aligned} \tau &= M(q)J(q)^\dagger(\ddot{x} - \dot{J}(q)\dot{q}) + C(q,\dot{q}) + G(q) \\ &= M(q)J(q)^\dagger(\ddot{x} - \ddot{x}_{bias}) \end{aligned} \tag{19}$$

Thus, Eq.(18) becomes

$$(\ddot{x} - \ddot{x}_{bias})^T (M(q)J(q)^\dagger)^T L^{-2} (M(q)J(q)^\dagger)(\ddot{x} - \ddot{x}_{bias}) \leq 1 \tag{20}$$

This equation is the de£nition of the Dynamic Manipulability Ellipsoid.

Next, we assume that $M_p \rightarrow \infty$. If we consider a stationary state ($\dot{x} = \ddot{x} = 0$) and ignore the effect of the gravity, Eq.(18) can be revised as

$$F_e^T J(q) L^{-2} J(q)^T F_e \leq 1 \tag{21}$$

This equation indicates the Manipulating-Force Ellipsoid.

Consequently, the IME is considered to have an intermediate nature between the DME and the MFE, and the DME and the MFE are both derived as limiting forms about the load mass. Though the idea for integrating the DME and the MFE for a particular task was proposed by Koeppe [2], their idea was based on the selection of both indexes obtained individually in task space. On the other hand, the proposed IME is a novel concept which includes both concepts of the DME and the MFE under the condition of a particular load mass.

E. Extension to Mass-Spring-Damper model

In some cases, the motion equation of the load held at the hand should be indicated by the following equation instead of Eq.(6) as shown in Fig.2 [9].

$$F_e = M_p \ddot{x} + C_p \dot{x} + K_p \Delta x + M_p \mathbf{g} \tag{22}$$

In this model, spring and damping characteristics at the contact point x are also considered. The proposed IME can take into account of these contact conditions while the DME cannot handle it. By taking these additional effects into consideration, Eqs. (8), (9), and (10) are rewriten as the following equations.

$$\tau = Q(q)(F_e - F'_{bias}) \tag{23}$$

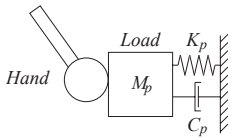

Fig. 2. Mass-Spring-Damper model

$$\begin{aligned} F'_{bias} &= (J(q)^T + M(q)J(q)^\dagger M_p^{-1})^\dagger \\ &\quad [M(q)J(q)^\dagger(\mathbf{g} + M_p^{-1}C_p\dot{x} + M_p^{-1}K_p\Delta x \\ &\quad + \dot{J}(q)\dot{q}) - C(q,\dot{q}) - G(q)] \end{aligned} \tag{24}$$

$$Q(q) = J(q)^T + M(q)J(q)^\dagger M_p^{-1} \tag{25}$$

Eq.(24) shows that spring and damping characteristics emerge in the bias term F'_{bias}.

III. Numerical examples

A. Design of an optimum leg structure for jump robots

In this section, we introduce a numerical example of the proposed impedance matching for determining an optimum leg posture for a 2-link jump robot.

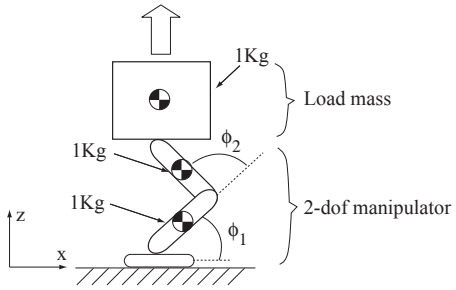

Fig. 3. Jumping robot

Let the length and the mass of each leg be 1[m] and 1[Kg], and the joint angles be ϕ_1 and ϕ_2, respectively. Fig.4 depicts the IME, the DME, and the MFE in the case that the body mass is 1[Kg], $\phi_1 = 45°, \phi_2 = 90°$, and maximum torque limit τ^{limit} is 10[Nm]. The unit of the IME and the MFE is $[N]$ and the unit of the DME is $[m^2/s]$.

Fig.4 shows that the IME is smaller than MFE since it includes the torque consumption in order to drive the mass of the manipulator itself. Moreover, the axis which indicates the highest torque-force transmission ef£ciency is given at the intermediate position between the one of the DME and the MFE. Thus, it can be said that the IME has an intermediate feature of these ellipsoids in terms of its shape.

Next, we compare the feasible output force toward the z direction for several initial postures. In this simulation, we assume that the sole is always placed under the center of the body, namely, $\phi_2 = \pi - 2\phi_1$. Figs.5 and 6 depict the values of IME and the DME in the z direction for several initial postures, respectively. Fig.5 shows that the proposed IME has a peak in transmission ef£ciency at $\phi_1 = 0.95[rad]$. On the other hand, the DME is monotonously decreasing as shown in Fig.6 since it doesn't take the body mass into account. Figs.7

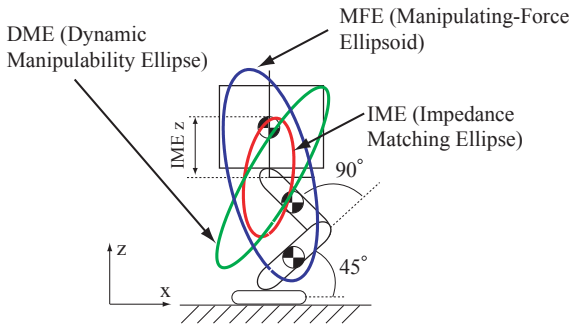

Fig. 4. Impedance matching ellipsoid, IME

and 8 depict the IME and the DME for 4 different leg postures. As straightening the legs, the distance of the DME in the z direction decreases monotonously. But the IME increases its distance at £rst, then begins to decrease.

The peak of the IME indicates the optimum posture in terms of torque-force transmission ef£ciency. Thus, this posture makes it possible to apply large force to the body even if the same joint torque is produced. Since the jumping height is determined by the time integral of the force applied to the body, the proposed IME indicates the performance of the link structure of the jump robot more correctly than the conventional indexes such as the DME or the MFE.

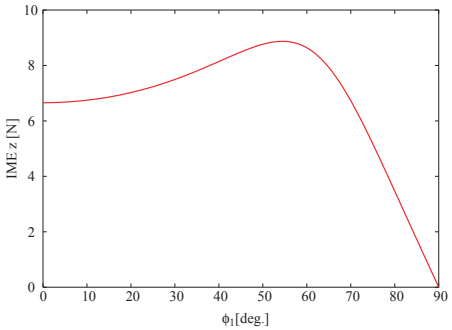

Fig. 5. Vertical force derived from IME

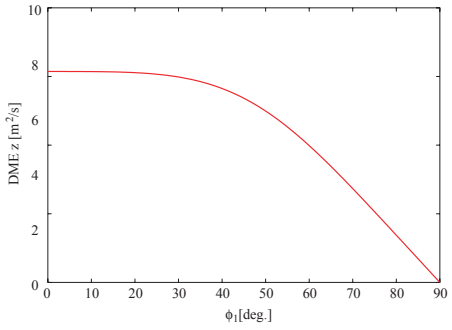

Fig. 6. Vertical acceleration derived from DME

We conducted jumping simulations of a 2-link jump robot using a dynamic simulator, OpenHRP. Length and mass of

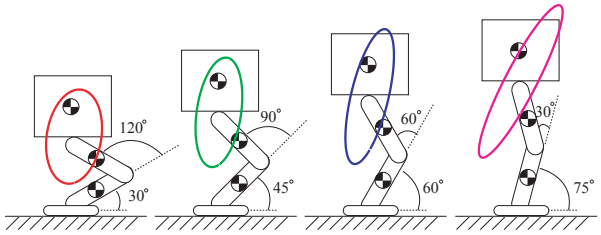

Fig. 7. IME for various leg postures

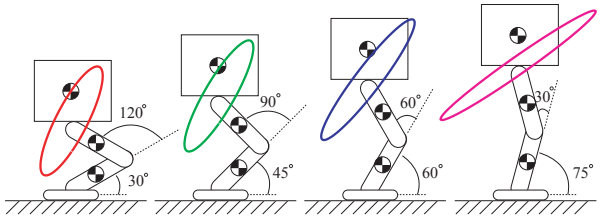

Fig. 8. DME for various leg postures

links are same as the model shown in Fig.3. In simulations, the torque of 300 [Nm] is applied to the joint 2 from 0 [sec] to 0.1 [sec], then the joint 2 is £xed after 0.1 [sec]. An example of simulation results in case of $\phi_1 = 50°$ is shown in Fig.9. Maximum jumping height, which is the distance from the height when the sole leaves the ground, to the maximum height, is depicted in Fig.10 for various leg postures. Maximum jumping height has a peak in case of $\phi_1 = 50°$ and it decreases rapidly if ϕ_1 increases. These results are very much in agreement with the expected results using the proposed IME as shown in Fig.5.

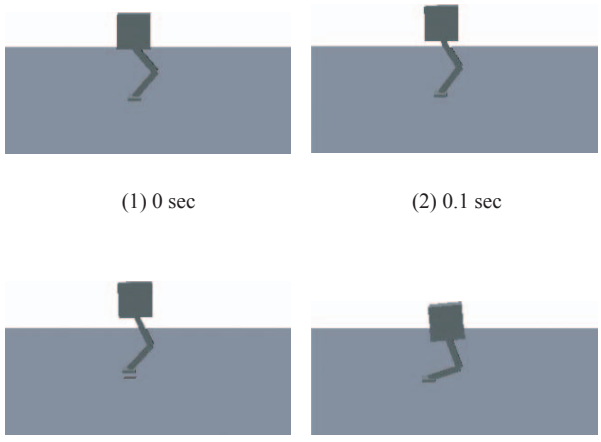

(1) 0 sec (2) 0.1 sec

(3) 0.26 sec (4) 1.0 sec

Fig. 9. An example of jumping simulation

B. Determinig optimum servo stiffness of active stiffness control for a serial link manuipulator

The IME, DME, and MFE of a typical serial link manipulator for assembly operation named PA-10 (Mitsubishi Heavy Industry, Inc.) are shown in Fig.11DThough the PA-10 consists

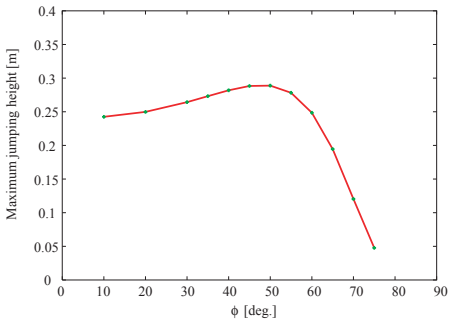

Fig. 10. Maximum jumping hight for various leg postures

of 7 joints including a rotational axis around an approach vector at hand, we omit this terminal joint and simplify it as a 6 dof manipulator. Total weight of the PA-10 is 32 Kg and a load mass grasped at hand is a 1Kg cubic-shape object with the width of 0.1m. Maximum joint torque is determined according to the speci£cation sheet.

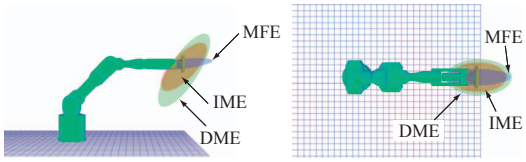

Fig. 11. Comparison of IME, DME, and MFE for 6-dof manipulator

The IME for various weight of the load mass are illustrated in Fig.12. The IME becomes small in the case that the load

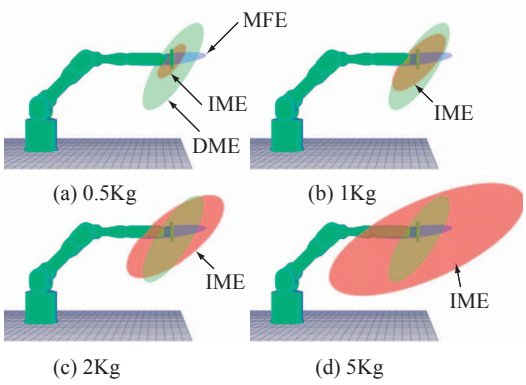

Fig. 12. Calculated IME for various load mass

mass is light since a majority of produced joint torque is consumed for the motion of the manipulator itself. On the other hand, the IME becomes large if the load mass gets heavy since most of the joint torque is transmitted to the load mass.

Active stiffness control[10] proposed in 1980s realizes impedance behavior of a manipulator hand by utilizing servo stiffness at each joint. In this method, the joint torque τ_i at the joint q_i is determined according to a deviation angle as

$$\tau_i = k_i \delta q_i \tag{26}$$

where k_i is servo stiffness at the joint i. When the desired stiffness at hand is shown as the following equation,

$$F_e = S\Delta x \tag{27}$$

the servo stiffness at each joint is obtained as

$$K = J^T S J \tag{28}$$

where $K = diag(k_1, k_2, \cdots, k_n)$. However, Eq.(28) doesn't consider the weight of the load mass nor the manipulator itself.

By taking both weight into consideration, the optimum servo stiffness for the active stiffness control, which realizes a desired impedance characteristic of the load, can be determined using the proposed IME. By substituting Eqs.(8) and (26) into Eq.(27), the optimum servo stiffness is calculated as

$$\begin{aligned} \tau &= QSJ\delta q - QF_{bias} \\ &= K\delta q + \tau_{bias} \end{aligned} \tag{29}$$

$$K = QSJ \tag{30}$$

Consequently, the load mass acquires the following impedance characteristic.

$$M_p\ddot{x} + S\Delta x = 0 \tag{31}$$

In the same manner, by choosing the servo stiffness and the viscosity term as

$$\begin{aligned} \tau &= QSJ\delta q + QCJ\dot{q} - QF_{bias} \\ &= K\delta q + D\dot{q} + \tau_{bias} \end{aligned} \tag{32}$$

the following impedance characteristic is obtained.

$$M_p\ddot{x} + C\dot{x} + S\Delta x = 0 \tag{33}$$

Examples in the cases of high stiffness to the approach and perpendicular directions are shown in Fig.(13).

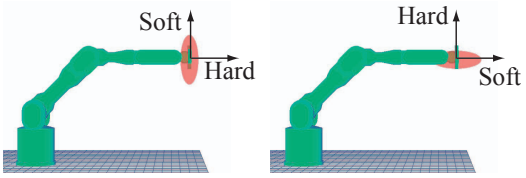

Fig. 13. Examples of IME for active stiffness control

C. The extension to a free ¤ying robot manipulator

The motion of manipulators mounted on a free ¤ying satellite in outer space causes the motion of the satellite itself due to the reaction force, since the ground to £x the foundation of the manipulator doesn't exist [11], [12]. Therefore, the mass of the manipulator affects the performance of operation ef£ciency more severely comparing with the manipulator on the ground. In this section, we introduce the extension of the proposed IME to free ¤ying robot manipulators.

Let's consider the free ¤ying robot with N joints and $N+1$ links. The mass and the tensor of inertia of each link are m_i

and I_i, respectively. The linear and angular momentum around the center of gravity of the robot are given as

$$\begin{pmatrix} P_g \\ L_g \end{pmatrix} = \begin{pmatrix} wI_3 & 0 \\ 0 & I_g \end{pmatrix} \begin{pmatrix} v_g \\ \omega_g \end{pmatrix} \tag{34}$$

where $w = \sum m_i$, $I_g = \sum I_i + m_i \tilde{r}_{gi} \tilde{r}_{gi}$, r_{gi} is a vector from the total center of gravity to the center of gravity of the link i, and $\tilde{r}$ is a skew]symmetric matrix. By differentiating Eq.(34), we get

$$\begin{pmatrix} \dot{P}_g \\ \dot{L}_g \end{pmatrix} = \begin{pmatrix} wI_3 & 0 \\ 0 & I_g \end{pmatrix} \begin{pmatrix} \dot{v}_g \\ \dot{\omega}_g \end{pmatrix} + \begin{pmatrix} 0 \\ \omega_g \times I_g \omega_g \end{pmatrix} \tag{35}$$

Moreover, there is a relationship between the force around the center of gravity and the force applied to the hand as follows:

$$\begin{pmatrix} f_g \\ n_g \end{pmatrix} = \begin{pmatrix} I_3 & 0 \\ \tilde{r}_{gh} & I_3 \end{pmatrix} \begin{pmatrix} f_h \\ n_h \end{pmatrix} \tag{36}$$

where $f_g = \dot{P}_g$ and $n_g = \dot{L}_g$.

Therefore, from Eqs.(35) and (36), the following equation can be obtained.

$$\begin{pmatrix} wI_3 & 0 \\ 0 & I_g \end{pmatrix} \begin{pmatrix} \dot{v}_g \\ \dot{\omega}_g \end{pmatrix} + \begin{pmatrix} 0 \\ \omega_g \times I_g \omega_g \end{pmatrix} = \begin{pmatrix} I_3 & 0 \\ \tilde{r}_{gh} & I_3 \end{pmatrix} \begin{pmatrix} f_h \\ n_h \end{pmatrix} \tag{37}$$

For convenience, we rewrite the above equation as

$$M\dot{V}_g + C = -R_h^T F_h \tag{38}$$

where $F_h = -(f_h, n_h)^T$ is force and moment applied from the hand to the load.

On the other hand, by using the generalized Jacobian matrix, J^*, for a free ¤ying robot proposed by Yoshida et al. [11], the following equation is valid between the velocity of the hand and the center of gravity, and the angular velocity at each joint.

$$V_h = J^* \dot{\phi} + R_h V_g \tag{39}$$

By solving Eq.(38) for F_h and substituting the derivative of Eq.(39), we get

$$F_h = -R_h^{-T} M R_h^{-1} \dot{V}_h + R_h^{-T} M R_h^{-1} J \ddot{\phi} \tag{40}$$

Here, we consider a stationary state and ignore the squared velocity term for simplicity.

In the case that a load with an inertial matrix W is being held at the hand, the force applied to the load is

$$F_h = W\dot{V}_h \tag{41}$$

From Eqs.(40) and (41), the acceleration of the hand is given as

$$\begin{aligned} \dot{V}_h &= (R_h^{-T} M R_h^{-1} + W)^{-1} R_h^{-T} M R_h^{-1} J^* \ddot{\phi} \\ &= SJ^* \ddot{\phi} \end{aligned} \tag{42}$$

Thus, the force applied to the load in Eq.(41) can be revised as

$$F_h = WSJ^* \ddot{\phi} \tag{43}$$

where $S = (R_h^{-T} M R_h^{-1} + W)^{-1} R_h^{-T} M R_h^{-1}$.

In general, the motion equation of a free ¤ying robot is given as

$$\tau = H^* \ddot{\phi} + C + J^{*T} F_h \tag{44}$$

Here, H^* is the tensor of inertia of the free ¤ying robot in joint space. By substituting Eq.(43) into Eq.(44), we get

$$\tau = (J^{*T} + H^* J^{*-1} S^{-1} W^{-1}) F_h \tag{45}$$

This equation indicates the joint torque which has to be produced for accelerating the load with the tensor of inertia, W, with the acceleration $\dot{V}_h$ given in Eq.(42). Thus, Eq.(45) is an extension of the impedance matching of serial link manipulators de£ned in Eq.(8) to free ¤ying robots.

Comparing Eq.(45) with Eq.(8) in the case that $\mathbf{g}$ and $\dot{q}$ are zero, we can £nd the following correspondences.

$$J \rightarrow J^* \tag{46}$$

$$M_p \rightarrow WS \tag{47}$$

Since S is a function of joint angles, the effect of the load W at the hand can be converted to the imaginary load WS for the free ¤ying robot, which changes according to the posture of the free ¤ying robot. For example, let's consider a task to catch a satellite in failure using a free ¤ying robot in outer space. By designing the optimum posture of the manipulator for catching the satellite in failure, the weight of the satellite in failure W can be changed to SW imaginary. Therefore, it is possible to reduce the torque required to catch the satellite and save the energy consumption. Conversely, if we consider a task to release a satellite from the free ¤ying robot to orbit, the satellite can receive a large releasing force with a small joint torque by choosing the optimum posture of the manipulator.

To verify the above discussion, we conduct computer simulations to release a child satellite using a 7-dof manipulator mounted on a free ¤ying satellite as shown in Fig.14. Here, we assume the size of a free ¤ying robot is 2m×2m×2m, the weight is 1000 Kg, and the length and the weight of each link are 1m and 10 Kg. The weight of the child satellite is 100 Kg.

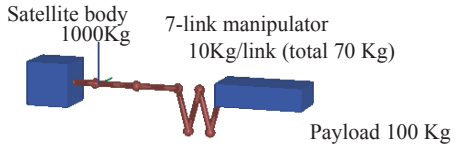

Fig. 14. 7-link manipulator on free ¤ying satellite

In the simulation, we examine 2 types of initial postures of 7-dof manipulator as shown in Fig.15, and measure the energy ef£ciency for releasing the child satellite toward x direction. The initial posture A indicates that the satellite-side links of the manipulator are folded and the initial posture B shows that the tip-side links are folded.

The IME for both initial postures are depicted in Fig.16. From these results, it can be estimated that the initial posture A has higher torque-force transmission ef£ciency regarding x direction than the initial posture B in a stationary state.

(a) Initial posture A

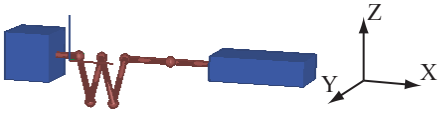

(b) Initial posture B

Fig. 15. Two initial postures

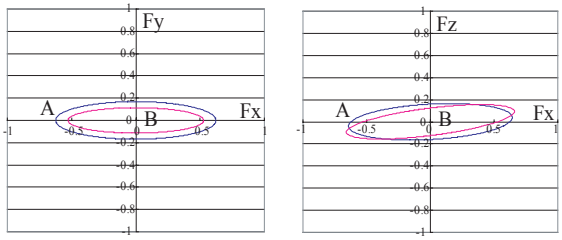

Fig. 16. Impedance matching ellipsoid

Next, torque-force transmission ef£ciency after accelerating the child satellite with $0.1m/s^2$ toward x direction is calculated. Fig.17 shows a ratio of the sum of joint torque produced at the joints and the sum of the force applied to the child satellite which has various weights. The results verify that the initial posture A has higher torque-force transmission ef£ciency than the initial posture B even after the manipulator moved.

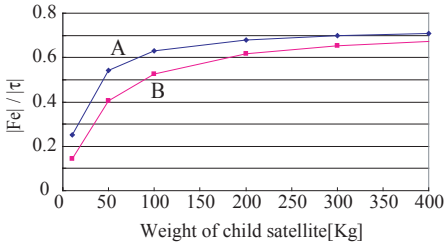

Fig. 17. Ef£cency of Torque-To-Force conversion

IV. CONCLUSIONS

In this paper, we propose a new index for dynamic performance analysis of serial link manipulators named Impedance Matching Ellipsoid, or IME.

The proposed IME indicates dynamic torque-force transmission ef£ciency from actuators at joints to a load held at a hand. The IME involves a wide range of concepts proposed so far as measures of manipulator's performance. The Dynamic Manipulability Ellipsoid (DME) and the Manipulating-Force Ellipsoid (MFE) are both derived from the IME as limiting forms about the load mass. In this paper, we demonstrate the IME with numerical examples including the selection of an optimal leg posture for a jump robot, and an extension for free ¤ying manipulators on satellites in outer space.

ACKNOWLEDGMENT

This research was partly supported by the 21st Century COE Program "Reconstruction of Social Infrastructure Related to Information Science and Electrical Engineering", and the Minsty of Public Management, Home Affairs, Posts and Telecommunications in Japan under Strategic Information and Communications R&D Promotion Programme (SCOPE).

REFERENCES

[1] T. Yoshikawa, "Manipulability of robot mechanisms," *The International Journal of Robotics Research*, vol. 4, no. 2, pp. 3–9, 1985.

[2] R. Koeppe and T. Yoshikawa, "Dynamic manipulability analysis of compliant motion," in *Proceedings of the IEEE/RSJ International Conference on Intelligent Robots and Systems '97*, 1997.

[3] S. L. Chiu, "Task compatibility of manioulator postures," *The International Journal of Robotics Research*, vol. 7, no. 5, pp. 13–21, 1988.

[4] T. Yoshikawa, "Dynamic manipulability of robot manipulators," *Journal of Robotics Systems*, vol. 2, no. 1, pp. 113–124, 1985.

[5] M. T. Rosenstein and R. A. Grupen, "Velocity-dependent dynamic manipulability," in *Proceedings of the IEEE International Conference on Robotics and Automation*, 2002.

[6] T. J. Graettinger and B. H. Krogh, "The acceleration radius: a grobal performance measure for robotic manipulators," in *Proceedings of the IEEE/RSJ International Conference on Intelligent Robots and Systems '88*, vol. 2, 1988, pp. 965–971.

[7] H. Asada, "A geomettrical representation of manipulator dynamics and its application to arm design," *Journal of Dynamic Systems, Measurement, and Control*, vol. 105, no. 3, pp. 131–135, 1983.

[8] R. Kurazume and T. Hasegawa, "Impedance matching for free ¤ying robots (in japanese)," in *The 20th Annual Conference of the Robotics Society of Japan*, 2002, p. 3J16.

[9] K. Yoshida and H. Nakanishi, "Impedance matching in capturing a satellite by a space robot," in *Proceedings of the 2003 IEEE/RSJ Intl. Conference on Intelligent Robots and Systems*, 2003, pp. 3059–3064.

[10] J. K. Salisbury, "Active stiffness control of a manipulator in cartesian coordinates," in *Proc. IEEE Conference on Decision and Control*, 1980, p. 102.

[11] Y. Umetani and K. Yoshida, "Continuous path control of space manipulators mounted on omv," *Acta Astronautica*, vol. 15, no. 12, pp. 981–986, 1987.

[12] K. Yoshida, R. Kurazume, N. Sashida, and Y. Umetani, "Modeling of collision dynamics for space free-¤oating links with extended generalized inertia tensor," in *Proc. IEEE Int. Conf. on Robotics and Automation*, 1992, pp. 889–904.